

# Design and Assembly of Modular Semi-Hemispherical Habitats for Mars using Dodecahedral Geometry

## Yuanqing Dai1\*

<sup>1</sup>Mountain View High School, Mountain View, CA, USA \*Corresponding Author: yuanqing.daidai08@gmail.com

Advisor: Dr. Dengfeng Sun, dsun@purdue.edu

Received November 1, 2024; Revised April 14, 2025; Accepted June 12, 2025

#### **Abstract**

The goal of this paper is to create a strategy for enabling effective and sustainable habitats on Mars's surface. To achieve this goal, a modular system is designed for the assembly of semi-hemispherical habitats utilizing dodecahedral geometry that has been proven to be structurally sound and efficient in materials. This research has three main parts. The first is the generation of a mathematical model to derive the desired panel dimensions for the specified habitat volume. The second is proposing a construction and assembly determination "devising mechanisms for construction" aimed at Mars in situ building. The design incorporates 3D-printed pentagonal and hexagonal panels which are easier to transport and assemble on Mars. The last part is verifying the designed techniques with the proposed scaled-down prototype model. The combination of modular design paired with in situ fabrication and ease of assembly creates an effective method to reduce materials needed to construct habitats, aiding in sustainable colonization of Mars.

Keywords: Aerospace and Aeronautical Engineering; Computation and Theory; Mars Habitat; Dodecahedron Structure; Addictive Manufacturing

#### 1. Introduction

Exploring and potentially settling Mars is one of the human's ambitious goals in the next decades. A key part of this challenge is creating habitats that can withstand the extreme conditions on Mars while being efficient and sustainable. The planet's thin atmosphere, severe temperature swings, and high levels of cosmic radiation require innovative designs that can keep inhabitants safe and make the best use of limited resources.

Various structures have been proposed for Mars habitats, each designed to address the unique environmental challenges of the planet (Cohen, 2015). One common design is the inflatable habitat, such as NASA's TransHab concept, which offers a lightweight, expandable structure that can be compacted for transport and then inflated on Mars to provide a pressurized living space (Kennedy, 2002; Zubrin et al., 2016). Another concept involves using underground or partially buried habitats to take advantage of Mars's regolith, a layer of loose and fragmented materials covering the surface of Mars, for natural insulation and radiation shielding (Lansdorp & Bengtson, 2009). For example, the Mars Ice House design proposes using water ice as a construction material, leveraging its abundance on Mars to create radiation-resistant walls (Ciardullo et al., 2016). The 3D printing of habitats using Martian regolith is another promising approach, as demonstrated by NASA's 3D Printed Habitat Challenge, where teams designed habitats that could be constructed on Mars using in-situ resources (Clinton et al., 2022). Additionally, geodesic domes, with their efficient material use and structural stability, have been considered a viable option for creating lightweight yet strong habitats that can withstand Mars's low atmospheric pressure and dust storms (Barker, 2008). Moreover, origaminspired engineering structures that can fit 3D curves have been introduced for constructing structures with unique shapes (Jing et al., 2024). While each of these designs presents innovative solutions, a comprehensive solution integrating all advantages, including transportability, material efficiency, and ease of construction remains unsolved.



A promising approach to addressing these challenges is the use of semi-hemispherical structures based on the geometry of a soccer ball, introduced by Eigil Nielsen in 1962 (Kotschick, 2006). The structure of the soccer ball is classified as a truncated icosahedron, which is a polyhedron with twenty faces. The soccer ball's arrangement of pentagons and hexagons provides structural integrity, while offering material efficiency (Chung & Sternberg, 1993). This truncated icosahedron structure provides a novel foundation for developing efficient Martian habitats (Murakami, 2001; Gelisgen, 2017; Kostant, 1995). This paper proposes a design for Mars habitats that leverages this geometric configuration to create a semi-hemispherical habitat, composed of assembable pentagonal and hexagonal panels (Hart, 2012), which can be easily assembled, disassembled, and transported.

The proposed design approach leads to several advantages. One, the soccer ball's semi-hemispherical shape provides optimal stress distribution, resulting in a lightweight yet strong structure. As the structure is required to sustain internal pressurization in a low-atmosphere environment (Rafkin et al., 2013) and resist potential damage from Martian dust storms, a semi-hemispherical shape has the potential to withstand extreme conditions. Two, pentagonal and hexagonal panels are modular, which makes them adaptable for additive manufacturing on Mars and enables compact transportation on the Martian surface. After reaching Mars, the straightforward assembly of the prefabricated panels eliminates the reliance on heavy machinery and intricate construction methods. Three, large-scale habitats can be built by linking several semi-hemispherical units together, which makes the modular approach feasible to facilitate large-scale construction.

To achieve the research goal, this paper outlines two key objectives: (1) Mathematical Modeling and Structural Design: Developing a mathematical model to calculate the volume of a semi-hemispherical habitat based on the soccer ball structure. This model ensures that the habitat meets specific volume requirements while determining the required material (area) when designing the semi-hemispherical habitats. A typical volume of 125 m³ is used for a prototype design. This volume provides sufficient space to support essential living zones of 1-2 astronauts. According to NASA's Human Integration Design Handbook (Allen et al., 2014), a minimum of 25–50 m³ per person is recommended for long-term missions. (2) 3D Printing and Assembly: Designing 3D-printed panels and assembly mechanisms that allow the modular panels to be easily assembled and dissembled. This fabricating and assembly strategy not only facilitates construction on Mars but also supports compact storage and transportation of the habitat construction materials from Earth to Mars. The two objectives outlined above are cohesively integrated to design and construct soccer ball-inspired habitats on Mars.

While the focus of this paper is on modeling and manufacturing of Mars habitat rooms, there is existing research on habitability and life support systems for Mars habitats, developed through NASA studies, like the Hawai'i space exploration analog and simulation mission (Binsted, 2015). The external structure design focused on this work can be integrated into internal life support systems. For example, internal segments can be adapted into zones for sleeping, working, and storage. In addition, the curved geometry allows for efficient air circulation, which can leverage existing air circulation systems on the ground embedded in curved-shaped stadiums. In follow-up studies, aspects for the long-term comfort, safety, and psychological well-being of crew members will be considered and integrated into the entire system design.

The remainder of this paper is organized as follows. The methods section includes the mathematical model of a semi-hemispherical structure based on the soccer ball and the 3D printing and assembly strategy. The simulation results and 3D printing prototype for one designed structure are demonstrated in the Results section. Discussion of the results and future research are addressed at the end.

#### 2. Materials and Methods

## 2.1 Mathematical Model and Design of Semi-Hemispherical Structure based on Soccer Ball

A soccer ball, shown in Figure 1 (a), is composed of 12 pentagons and 20 hexagons with equable side lengths, where each pentagon is surrounded by five hexagons. A semi-hemispherical habitat that leverages the soccer ball structure is composed of part of the pentagons and hexagons. As shown in Figure 1 (b), 6 pentagons, 5 hexagons, and 5 half hexagons are used to constitute a semi-hemispherical habitat. When approximating the soccer ball as a perfect sphere, its volume is calculated as  $V = \frac{4}{3}\pi r^3$ , where r is the radius of the sphere. However, an exact soccer ball



structure truncates 32 faces to generate the so-called truncated icosahedron, yielding 12 regular pentagons and 20 regular hexagons. The volume of the truncated icosahedron that excludes the truncated vertices is determined by  $V = \frac{125+43\sqrt{5}}{4}a^3$ , where a is the edge length (Berman, 1971). The semi-hemispherical habitat is treated as the stacking of three frustums, shown in Figure 1 (c). Each frustum is the portion of a pyramid that lies between two parallel planes after removing the upper part. The bases of the three frustums are highlighted, and then an approach is proposed to calculate the volume of the semi-hemisphere by finding the volume of each frustum. This approach allows us to find not only the exact volume of the semi-hemisphere but also the location of each vertex.

The volume of a frustum is calculated by

$$V = \frac{1}{3} height(top\ area + bottom\ area + \sqrt{top\ area \times bottom\ area}) \tag{1}$$

Based on this formula, the modeling section focuses on finding the height, top surface area, and bottom surface area for each frustum to calculate its volume. This principle guides the computation of the following steps. Since the surface areas and height of each frustum are not directly available, the properties of a soccer ball structure, combined with geometry relationships, are utilized to find necessary items for calculating each frustum volume.

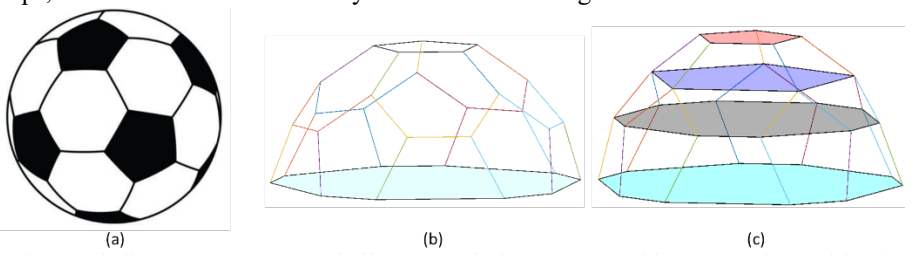


Figure 1: Illustration of soccer ball structure, (a) soccer ball composed of pentagons and hexagons, (b) semi-hemispherical habitat based on soccer ball structure, and (c) three stacked frustums in the semi-hemispherical habitat.

Starting from the top frustum in Figure 2 (a), where its top and bottom bases are both pentagons, the volume of the top frustum is calculated by

$$V_t = \frac{1}{3}h_1(A_1 + A_2 + \sqrt{A_1 \times A_2}) \tag{2}$$

where  $A_1$  and  $A_2$  are the areas of the top and bottom bases, respectively, and  $h_1$  is the vertical distance between the top and bottom bases. For the regular pentagon and hexagon surfaces considered in the soccer ball, it is assumed that their side length is denoted by a. Then the top base area  $A_1 = \frac{5}{4}\cot\left(\frac{\pi}{5}\right)a^2$ . The side of the bottom pentagon is the cross arc of the longest diagonal of the hexagon with length 2a. Thus, its area  $A_2 = 5\cot\left(\frac{\pi}{5}\right)a^2$ . Using the geometry relationship in Figure 2 (b), the height of the top frustum is determined by  $h_1 = \sqrt{s^2 - d_1^2}$ , where  $s = \frac{\sqrt{3}}{2}a$  and  $d_1 = \frac{1}{2}\cot\left(\frac{\pi}{5}\right)a$ . To facilitate the calculation of the following frustum models, the Cartesian coordinate is used where the top pentagon base is located in the horizontal x-y plane with one of the vertices located at the origin, denoted by  $t_1(0,0,0)$ , and another vertex located at  $t_2(a,0,0)$ , along the x-axis. Then the center of the top pentagon is located at

 $t_c(\frac{1}{2}a,\frac{1}{2}\cot(\frac{\pi}{5})a,0)$ . Moreover, the coordinate of the bottom pentagon vertex,  $p_1$ , that is connected to  $t_1$ , is determined. By finding the distance from  $p_1$  to the projected point of  $t_1$  on the bottom pentagon, denoted by  $d_2 = \sqrt{a^2 - h_1^2}$ , the coordinate of  $p_1$  is then determined by  $p_1(-\cos(\alpha)d_2, -\sin(\alpha)d_2, -h_1)$ , where  $\alpha = \arccos(\frac{a}{2d\alpha})$ .

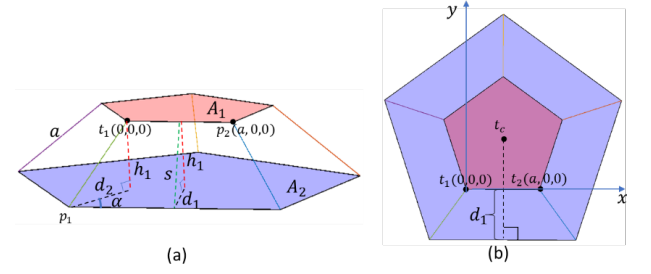


Figure 2: Geometry of the top frustum, (a) side view, and (b) top view.

For the middle frustum shown in Figure 3 (a), its top base is the bottom base of the top frustum, which is a regular



pentagon with side length 2a, while its bottom base is a polygon with sides composed of hexagon sides and diagonals of a pentagon. The height of the middle frustum, denoted by  $h_2$ , is the same as the height of the top frustum, i.e.,  $h_2 = h_1$ . This is because the bottom base of the top frustum is composed of the longest diagonal of the hexagon, resulting in the equal vertical distance to the top base of the top frustum and bottom base of the middle frustum. Then the coordinate of the bottom base vertex connecting to  $p_1$  is determined by  $m_1(0, -2sin(\alpha)p, -2h_1)$ . Moreover, the center of the bottom base coordinate,  $m_c\left(\frac{1}{2}a, \frac{1}{2}\cot\left(\frac{\pi}{5}\right)a, -2h_1\right)$ , is detrimined. Now, the radius of the bottom base from the center  $m_c$  to any vertex, can be determined by  $r_m = ||m_1 - m_c||_2$ , where  $||.||_2$  represents the two norm of a vector. The bottom base of the middle frustum can be regarded as the composition of two types of isosceles triangles, denoted by  $T_1$  and  $T_2$  in Figure 3 (b), both having leg lengths of  $r_m$ . The base length of of triangle  $T_1$  is a and the one for triangle  $T_2$  is  $2cos(\frac{\pi}{5})a$ . As the bottom base of the middle frustum is composed of  $5T_1$  and  $5T_2$ , its area can be

determined by  $A_3 = \frac{5}{2} tan(\beta_1)a^2 + 5cos\left(\frac{\pi}{5}\right)tan(\beta_2)a^2$ , where  $\beta_1 = \arcsin\left(\frac{a}{2r_m}\right)$  and  $\beta_2 = \arcsin\left(\frac{cos(\frac{\pi}{5})a}{r_m}\right)$ . Similar to Equation (1), the volume of the middle frustum is determined by  $V_m = \frac{1}{3}h_2(A_2 + A_3 + \sqrt{A_2 \times A_3})$ .

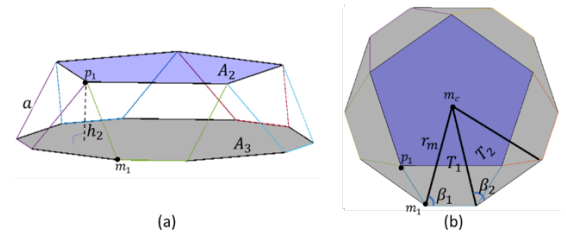


Figure 3: Geometry of the middle frustum, (a) side view, and (b) top view.

The bottom frustum is shown in Figure 4 (a), where its top base is the bottom base of the middle frustum, while its bottom base is a polygon with sides composed of 5 pentagon sides and longest diagonals of 5 hexagons. The vertex  $p_1$  is projected on the top base and bottom base of the bottom frustum. The distances from  $p_1$  to the two bases are denoted by  $h_2$  and  $h_2 + h_3$ , respectively, where  $h_2 = h_1$ , as stated above, and  $h_3$  is the height of the bottom frustum. Now another project of  $p_1$  on its

opposite side of the red pentagon is made, shown in Figure 4 (a). The distance from  $p_1$  to its opposite diagonal line and the opposite side of the red pentagon is denoted by  $s_2$  and  $s_2'$ , respectively, where  $s_2 = cos(\frac{\pi}{5})a$  and  $s_2' = s_2 + cos(\frac{\pi}{5})a$ 

 $arcsin\left(cos\left(\frac{\pi}{5}\right)-\frac{1}{2}\right)a$ . Since  $\frac{s_2}{s_2'}=\frac{h_2}{h_2+h_3}$ , it leads to  $h_3=\frac{cos\left(\frac{\pi}{5}\right)}{arcsin\left(cos\left(\frac{\pi}{5}\right)-\frac{1}{2}\right)}h_2$ . Then, the center of the bottom base coordinate is determined by  $b_c\left(\frac{1}{2}a,\frac{1}{2}\cot\left(\frac{\pi}{5}\right)a,-2h_1-h_3\right)$ . Next, the focus is on finding the coordinate of the bottom base vertex connecting to  $m_1$ , denoted by  $b_1$ . Within the red pentagon, the vector  $\overline{p_1m_1}$  is parallel to the vector  $\overline{m_2b_1}$ . Thus, it leads to the ratio  $\frac{\|m_2-b_1\|_2}{\|p_1-m_1\|_2}=\frac{(m_2-b_1)y}{(p_1-m_1)y}$ , where the subscript y denotes the y-component of a vector. Since  $\|m_2-b_1\|_2=2cos\left(\frac{\pi}{5}\right)a$ ,  $\|p_1-m_1\|_2=a$ , and  $(p_1-m_1)_y=sin(\alpha)d_2$ , it indicates that  $(m_2-b_1)_y=2cos\left(\frac{\pi}{5}\right)sin(\alpha)d_2$ . The coordinate of  $m_2$  can be found from the coordinates of  $m_1$  and the two isosceles angles  $\beta_1$  and  $\beta_2$ , expressed as  $m_2\left(-2cos\left(\frac{\pi}{5}\right)cos(\beta_1+\beta_2)a, -2sin(\alpha)p+2cos\left(\frac{\pi}{5}\right)sin(\beta_1+\beta_2)a, -2h_1\right)$ . Then, the coordinate of  $b_1$  is determined by  $b_1\left(-cos(\alpha)d_2, -2sin(\alpha)p+2cos\left(\frac{\pi}{5}\right)sin(\beta_1+\beta_2)a, -2h_1\right)$ .

 $2cos\left(\frac{\pi}{5}\right)sin(\alpha)d_2$ ,  $-2h_1-h_3$ ). Now, the radius of the bottom base can be determined by calculating the two norm of the difference between the center  $b_c$  to vertex  $b_1$ , denoted by  $r_b = \|b_1 - b_c\|_2$ . Similar to the calculation of  $A_3$ , the calculation of the bottom base area of the bottom frustum, denoted by  $A_4$ , is composed of  $5T_3$  and  $5T_4$ , where  $T_3$  and  $T_4$  are areas of two isosceles triangles, shown in Figure 4 (b). Then the bottom base of the bottom frustum is determined by  $A_4 = \frac{5}{2}cos(\gamma_1)a^2 + 5cos\left(\frac{\pi}{5}\right)cos(\gamma_2)a^2$ ,

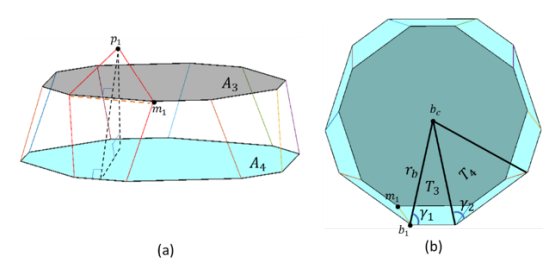


Figure 4: Geometry of the bottom frustum, (a) side view, and (b) top view.



where  $\gamma_1 = \arcsin\left(\frac{a}{2r_b}\right)$  and  $\gamma_2 = \arcsin\left(\frac{a}{r_b}\right)$ . Similar to Equation (1), the volume of the bottom frustum is determined by  $V_b = \frac{1}{3}h_3\left(A_3 + A_4 + \sqrt{A_3 \times A_4}\right)$ .

The overall semi-hemispherical habitat can be determined by

$$V = V_t + V_m + V_b = 28.032a^3 (3)$$

This volume model leads to the exact analytical solution without approximation, which allows us to find the precise habitat volume when the side length a is given. In addition, the area of the 6 pentagons, 5 hexagons, and 5 half hexagons that constitute the semi-hemispherical habitat is determined by

$$S = \left(7.5 \frac{3}{2} \sqrt{3} + 6 \frac{5}{4} \sqrt{1 + \frac{2}{\sqrt{5}}}\right) a^2 \tag{4}$$

Conversely, for a structure with a given volume, the required side length a can be determined by using the volume formula and then the area for constructing the habitat can also be determined, which indicates that the materials needed for building such a habitat can be estimated accordingly.

## 2.2 Additive Manufacturing and Assembly Approach

The design of the Mars semi-hemispherical habitat is based on a scalable and efficient additive manufacturing method. In this part, the Mars habitat's construction materials will be presented first, then the assembly methods will be described, including the assembly mechanism and the process of fabricating the habitat's modular components.

For constructing the modular components, two materials were chosen; Thermoplastic Polyurethane (TPU) and Polylactic Acid (PLA), which provide flexibility while maintaining structural strength. In the assembly of the hexagonal panels, adjustment fitting of hexagons is made easier by manufacturing the hexagonal panels from TPU, a versatile 3D printing material. The hexagonal wings manufactured from TPU can deform slightly and slide smoothly into the slots designed in the pentagonal panels. On the other hand, known for rigidity, PLA is used to fabricate the pentagonal panels. The rigid nature of PLA allows the pentagons to work as the primary load-bearing elements of the structure, as they provide strength to the overall shape and stability of the habitat. Nonetheless, real Mars applications require materials with the ability to withstand harsh and extreme temperatures, substantial radiation, and mechanical stress. For future implementation, space-grade elastomers such as silicone-based polymers (Nair et al., 2017) could replace TPU for the flexible components. Similarly, high-performance composite materials such as carbon fiber-reinforced polymers (Anvari, 2017), could serve as alternatives to PLA for the rigid load-bearing panels. Thus, TPU and PLA in this study are selected to replicate the mechanical behavior of more advanced materials to save cost and make accessibility easy.

The assembly mechanism leverages a sliding mechanism that connects the hexagons to the pentagons. As shown in Figure 1 (a), each pentagonal panel has five sides, where each side is adjacent to a hexagonal panel in the truncated icosahedron structure. To attach five hexagons to each side of a pentagon, a slot is designed along the edge of each pentagonal side, as shown in the CAD model of Figure 5 (a). With these designed slots, the raised bars from the hexagonal panels can be securely slid into place, and then tightly lock the components together. To ensure a tight and stable fit, the dimensions of the pentagonal slots are designed to match the raised bars on the hexagons. Each hexagonal panel is designed with three wings on every other side, all equipped with raised bars. These bars fit into the

corresponding slots on the pentagonal panels. The flexibility of the TPU material allows the wings to be foldable and can be slid into place while maintaining enough elasticity to ensure the panels are securely fastened once assembled. The CAD model in Figure 5 (b) illustrates the precise placement of these wings and the raised bars that facilitate the assembly.

The modular components are fabricated using a Prusa XL 3D printer that is capable of producing high-

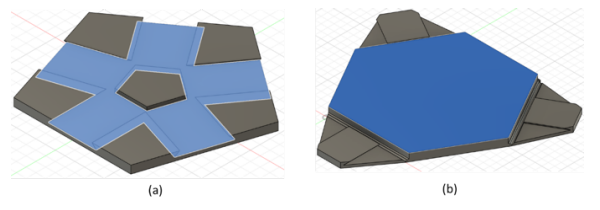
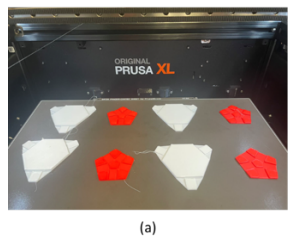


Figure 5: CAD design of the pentagon and hexagon panels, (a) bottom surface of a pentagon with five slots, and (b) bottom surface of a hexagon with three wings.



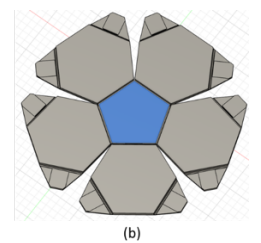


Figure 6: Fabrication and assembly of modular parts, (a) components fabricated from a 3D printer, and (b) one pentagon assembled with five hexagons.

quality, large-scale prints with precision, as shown in Figure 6 (a). Once printed, the components are easily assembled. As demonstrated in Figure 6 (b), a single pentagonal panel can be connected to five surrounding hexagonal panels by sliding the foldable wings of each hexagon into the corresponding slots on the pentagon. This assembly process requires minimal tools and effort, as the TPU's flexibility allows for straightforward adjustment during fitting, and the rigid PLA pentagons lock the panels into a stable configuration. The result is a robust, modular

structure that can be quickly assembled on-site, making it highly suitable for the challenging environment of Mars.

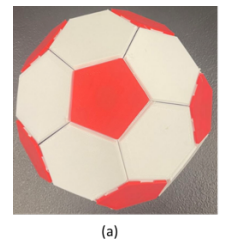
#### 3. Results

In this section, the results of the habitat design calculations and the corresponding 3D-printed prototype were presented. First, the mathematical model was developed to compute the volume of the semi-hemispherical structure, based on the truncated icosahedron geometry, which was used to determine the required dimensions of the pentagonal and hexagonal panels. Then, the 3D printing and assembly of a scaled-down prototype of the habitat were presented.

The example provided here was to achieve a habitat volume of 125 m<sup>3</sup>. The mathematical model developed in the earlier sections was applied. According to Equation (3), the side length a = 1.646 m was determined to construct such a habitat room. In addition, according to Equation (4), the overall area S = 80.765 m<sup>2</sup> was determined. However, when constructing a traditional hemispherical habitat room, its volume and area are determined by  $\frac{2}{3}\pi r_h^3$  and by  $2\pi r_h^2$ , respectively, where  $r_h$  is the radius of the hemisphere. Thus it requires an overall area of 95.95 m<sup>2</sup> to construct a traditional hemispherical habitat room with the same volume. The material savings using the truncated icosahedron structure for constructing the same volume of habitat room validate its efficiency. Moreover, internal room pressure

or curved frames are required to maintain the traditional hemispherical shape, which is not required for the proposed truncated icosahedron structure using the interlocking assembly approach.

To validate the assembly process and material performance, a scaled-down prototype of the semi-hemispherical habitat was fabricated using 3D printing. The Prusa XL 3D printer was used to create individual pentagonal and hexagonal panels, as discussed in the manufacturing approach section. The prototype of an assembled habitat room is shown in Figure 7.



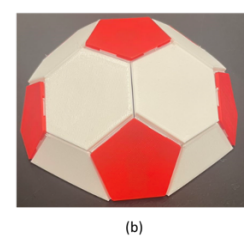


Figure 7: Prototype of an assembled habitat room, (a) top view, and (b) side view.

## 4. Discussion

Through the development of the mathematical model, the precise side lengths of the pentagons and hexagons required to construct a habitat with a given volume can be determined. The combination of hybrid material 3D printing technology and sliding assembly mechanism generated a feasible approach for fabricating the designed habitats on Mars. The construction of the scaled-down prototype validated the feasibility of the proposed design and construction approach. The modular design, using flexible and rigid materials for the hexagons and pentagons respectively, proved effective in creating a structure that is both easy to assemble and sturdy once completed. The sliding wing and slot mechanism ensured secure connections between panels while allowing for disassembly if needed. As the materials and manufacturing process used in the prototype can be directly applied to the larger habitat structure, this scaled-down prototype also provided a proof-of-concept for the full-scale habitat. For a large-size habitat, the three frustums shown in Figure 1 (c) naturally divided the structure into three layers when floors were installed for the top and middle frustums. The capability to easily divide the habitat into multiple layers based on the three frustums added



functionality to the proposed habitats to meet different size/space/usage requirements from users. In summary, the proposed design offered several key advantages: efficient use of materials, ease of assembly and disassembly, and adaptability to future exploration missions.

The design and 3D printing process can be fully autonomous when integrating the design with the 3D printing software to reduce human efforts. The only step that requires human interaction is the assembly process. As robotic assembly lines, equipped with end efforts to manipulate and sense objects, have been applied to massive production and assembly in the industry, future work will consider adopting robotic arms for autonomous assembly. In addition, the extreme conditions, such as radiation and extreme temperature changes, will affect the durability of Mars habitats. Considering these environmental challenges, future research will also investigate specific materials to withstand Martian environmental factors in long-term missions.

#### 5 Conclusion

This study establishes that habitats for Mars can be constructed through modular pentagon and hexagon panels using the truncated icosahedron geometry, commonly seen in a soccer ball. The approach enables cost-efficient, robust, and transportable habitation, which is suitable for sustainable human colonization on Mars. A mathematical model was developed to determine the necessary panel dimensions for achieving a specific internal volume. A comparison of material usage between the proposed structure and traditional hemispherical structure validates the material savings using the proposed approach. Easily accessible additive manufacturing materials were used to build a scaled-down prototype, where flexible hexagonal panels were produced using thermoplastic polyurethane (TPU), while rigid pentagonal panels were printed using polylactic acid (PLA). The interlocking assembly method based on raised bars and matching slots enabled fast and secure construction without specialized tools. The broader significance of this research lies in its demonstration of a low-complexity, material-efficient, and highly modular construction approach for Mars surface habitats.

However, several limitations remain that will be addressed in future work. First, the current design focuses on geometric configuration and external structure assembly, which has not been integrated into critical life support systems such as air circulation, thermal control, pressure regulation, or radiation shielding. Second, the materials used for the prototype, TPU and PLA, focus on cost-effectiveness and accessibility during the early-stage design and prototyping development, which are not viable under actual Mars extreme conditions. More durable aerospace-qualified materials would be required for practical applications. Third, the structural properties of the assembled habitat under Martian gravity, internal pressurization, and external loads will be analyzed in future work. The limitations lay the future directions that will integrate comprehensive design components to make the Mars habitat room more feasible, efficient, and robust.

## Acknowledgment

I want to thank Prof. Dengfeng Sun in the School of Aeronautics and Astronautics at Purdue University for his guidance throughout my research process.

### References

Allen, C., et al. (2014). NASA Human Integration Design Handbook, NASA/SP-2010-3407/REV1.

Anvari, A. (2017). Fatigue life prediction of unidirectional carbon Fiber/epoxy composite on Mars. *Journal of Chemical Engineering and Materials Science*, 8(8), 74-100. https://doi.org/10.5897/JCEMS2017.0303

Barker, D. (2008). Solar System Longboats: A Holistic and Robust Mars Exploration Architecture Design Study. *AIAA SPACE 2008 Conference & Exposition*. San Diego, California. https://doi.org/10.2514/6.2008-7881

Battalio, M. and Wang, H. (2021). The Mars Dust Activity Database (MDAD): A comprehensive statistical study of dust storm sequences. *Icarus*, 354, p.114059. https://doi.org/10.1016/j.icarus.2020.114059



Berman, M. (1971). Regular-faced convex polyhedra. *Journal of the Franklin Institute*, 291(5), 329-336. https://doi.org/10.1016/0016-0032(71)90071-8

Binsted, K. (2015). Hawai'i Space Exploration Analog and Simulation. http://hdl.handle.net/10125/37427

Ciardullo, C., et al. (2016, July). Mars ice house: using the physics of phase change in 3D printing a habitat with H2O. In *The 46th International Conference on Environmental Systems was held in Vienna, Austria,* 2016.

Chung, F., & Sternberg, S. (1993). Mathematics and the Buckyball. *American scientist*, 81(1), 56-71. https://www.jstor.org/stable/29774821

Clinton, R. G., et al. (2022). NASA's Moon-to-Mars Planetary Autonomous Construction Technology Project: Overview and Status. 73rd International Astronautical Congress (IAC). Paris.

Cohen, M. M. (2015). First Mars habitat architecture. *AIAA SPACE conference and exposition*. Pasadena, California. https://doi.org/10.2514/6.2015-4517

Gelisgen, Ö., Ermis, T., & Gunaltılı, I. (2017). A note about the metrics induced by truncated dodecahedron and truncated icosahedron. *International Journal of Geometry* 6(2), 5-16.

Hart, G. (2012). Goldberg polyhedra. In Shaping space: Exploring polyhedra in nature, art, and the geometrical imagination (pp. 125-138). New York, NY: Springer New York. https://doi.org/10.1007/978-0-387-92714-5

Huang, C. H., et al. (2011). Study of the temperature flow field change by air-conditioning system in a indoor circular stadium. IEEE International Conference on Consumer Electronics, Communications and Networks, Xianning, China, https://doi.org/10.1109/CECNET.2011.5769320

Jing, G., et al. (2024). Design and Transformation Control of Triangulated Origami Tessellation: A Network Perspective. *IEEE Transactions on Network Science and Engineering*, 11(1), 635 - 647. https://doi.org/10.1109/TNSE.2023.3303260

Kennedy, K. (2002). Lessons from TransHab: An Architect's Experience. *AIAA Space Architecture Symposium*. Houston, Texas. https://doi.org/10.2514/6.2002-6105

Kostant, B. (1995). The graph of the truncated icosahedron and the last letter of Galois. *Notices American Mathematical Society*, 42(9), 8-16. https://doi.org/10.1515/dmvm-1995-0405

Kotschick, D. (2006). The topology and combinatorics of soccer balls: when mathematicians think about soccer balls, the number of possible designs quickly multiplies. *American Scientist*, 94(4), 350-357. https://www.jstor.org/stable/27858804

Lansdorp, B., & Bengtson, K. V. (2009). Mars Habitat Using Locally Produced Materials. *In Out of This World: The New Field of Space Architecture* (pp. 311-315). AIAA. https://doi.org/10.2514/5.9781563479878.0311.0315

Murakami, H., & Nishimura, Y. (2001). Static and dynamic characterization of regular truncated icosahedral and dodecahedral tensegrity modules. *International Journal of Solids and Structures* 38(50-51): 9359-9381. https://doi.org/10.1016/S0020-7683(01)00030-0

Nair, S., et al. (2017). Studies on the thermal properties of silicone polymer-based thermal protection systems for space applications. *Journal of Thermal Analysis and Calorimetry*, 128, 1731-1741. https://doi.org/10.1007/s10973-016-6025-2

Rafkin, S. C. R., et al. (2013). Mars: Atmosphere and climate overview. *In Comparative climatology of terrestrial planets*, (pp. 55-89). https://doi.org/10.2458/azu\_uapress\_9780816530595-ch003.

Zubrin, R., Baker, D., & Gwynne, O. (1991). Mars direct-a simple, robust, and cost effective architecture for the space exploration initiative. *29th Aerospace Sciences Meeting*. Washington, D. C. https://doi.org/10.2514/6.1991-329